This is a repository copy of *Investigating the effect of glass filler on the aging behavior of polymer powders for additive manufacturing*.

White Rose Research Online URL for this paper:
https://eprints.whiterose.ac.uk/id/eprint/229563/

Version: Published Version

eprints@whiterose.ac.uk
https://eprints.whiterose.ac.uk/

Investigating the effect of glass filler on the aging behavior of polymer powders for additive manufacturing

John Duffy, Serena Agostini, Ryan Brown, Candice Majewski, Shona Marsh & Natalie Rudolph

View supplementary material ⬀

Published online: 09 Jul 2025.

Submit your article to this journal ⬀

Article views: 91

View related articles ⬀

View Crossmark data ⬀

Taylor & Francis
Taylor & Francis Group

Investigating the effect of glass filler on the aging behavior of polymer powders for additive manufacturing

John Duffy[a], Serena Agostini[a], Ryan Brown[b], Candice Majewski[c] ⓘD,
Shona Marsh[d] and Natalie Rudolph[e]

[a]Malvern Panalytical Ltd, Worcestershire Malvern, UK; [b]Multidisciplinary Engineering Education, University of Sheffield, Sheffield, UK; [c]School of Mechanical, Aerospace and Civil Engineering, University of Sheffield, Sheffield, UK; [d]Netzsch Thermal Instruments UK Ltd, Unit 6 Element Court, Wolverhampton, UK; [e]NETZSCH-Gerätebau GmbH, Selb, Germany

ABSTRACT

Powdered-polymer additive manufacturing processes, including selective laser sintering, high-speed sintering, and multijet fusion, have seen increasing usage throughout a range of industries, with corresponding requirements for better knowledge of material and component behavior. These processes involve the preheating, and subsequent selective melting, of consecutive layers of powder. Upon completion of the manufacturing process, unmelted powder can be recovered from the build chamber and, depending on its quality, reused for future part manufacture. Powder recovered in such a way can undergo a number of changes as a result of being held at elevated temperatures for extended times during the manufacturing process. Previous research has investigated these effects for polymer powders, with a particular emphasis on the most common polymer additive manufacturing powder, Nylon-12. In this work, we use a variety of characterization techniques, specifically size exclusion chromatography, differential scanning calorimetry, and rotational rheometry, to investigate this behavior for a glass-filled nylon-12 material, in order to identify any effects of the glass filler on material changes and on the properties of parts produced using these materials.

Introduction

Powdered-polymer additive manufacturing (AM) processes, including selective laser sintering (SLS), high speed sintering (HSS), multijet fusion (MJF), and selective absorption fusion (SAF), are receiving increasing interest from industry, in large part due to the additional geometric complexity they can provide compared with other polymer AM processes. Polymer powders also brought the highest revenue among AM materials in 2024.[1] During these processes, cross-sections of preheated polymer powder are melted in a layer-by-layer manner until the part or parts are complete. Upon completion of the AM process, parts are removed from the build chamber, and the unmelted powder surrounding them is captured for reuse or disposal. From both a sustainability and a financial perspective, it is preferable to reuse as much of the unmelted powder as possible for use in subsequent builds, with a 70–30 ratio of used to fresh powder being somewhat standard practice in SLS.

Significant amounts of research have been conducted into the changes encountered in this unmelted powder, in particular for nylon-12, the highly dominant material in the powdered-polymer AM market.

Early work in this area[2] demonstrated that the melt flow rate (MFR) of nylon-12 decreased in powder recovered from successive SLS builds, suggesting an increase in molecular weight. Later research[3] replicated similar effects using a combination of recovered powder and powder that had been artificially aged, demonstrating that MFR decreased most at higher temperatures and after longer times, and proposing a powder reuse strategy based on the MFR of recovered powder from different regions of the build chamber.

Subsequent work has developed a deeper understanding of this behavior. Wudy and Drummer[4] used gel permeation chromatography to demonstrate linear macromolecular growth with thermal aging, proposing post-condensation as the dominant mechanism. Oven conditioning in air[5] indicated that, beyond a certain point of aging, thermo-oxidative degradation became the dominant aging process, with corresponding deterioration in mechanical behavior of hot-pressed test samples.

Other work has investigated the effects of thermal aging on different polymers. Pandelidi et al.[6] investigated the aging of nylon-11, demonstrating that properties of powder and of compression-molded specimens produced from this powder changed significantly within the first 24 h of exposure to elevated temperature, but that consecutive exposure did not have a significant effect. Stiller et al.[7] demonstrated an increase in powder viscosity for nylon-6 following SLS successive builds, with the most significant effect observed upon first heating. Williams et al.[8] showed that polypropylene could be reused through multiple cycles of the HSS process with little-to-no detriment to tensile properties and no apparent change in polymer chemistry as inferred from molecular weight data.

The vast majority of existing research has focused on investigating thermal aging of 'pure' polymer powders. However, a number of filled polymer powders are used in the AM industry in order to expand the range of properties achievable through powdered-polymer AM; one of the most dominant of these is glass-filled nylon. It is possible that the inclusion of fillers may lead to changes in the behavior of the base polymer, for example, due to changes in energy absorption and/or heat transfer characteristics or through the use of chemicals involved in the filler production or mixing processes. In this work, we provide a comprehensive characterization of a glass-filled and unfilled nylon-12 material in order to identify any effects of the glass filler on the aging behavior of the polymer. We then correlate these changes with the tensile properties of parts produced using the HSS process.

Methods

Material selection and preparation

Two materials were selected for this study: a glass-filled and unfilled nylon-12 (PA615-GS and PA650, respectively), produced by Advanced Laser Materials and supplied by RP Support Ltd. Powder aging was carried out in an MMM Group Vacucell oven, Model BUK-B2V-M/VU22, and conducted in a nitrogen atmosphere in order to remove any possible oxidative effects that might occur when heating in air. For safety purposes, the oven was housed in a fume cupboard for the duration of the aging process. Powder was aged in metal trays, using 1 kg quantities in approximately 25 mm layers. The following heating cycle was used for all powders once nitrogen purging was complete:

- Powder heated from room temperature to 170 °C over a 1 h period.
- Powders held at 170 °C for 24 or 96 h.
- Heaters switched off and powders allowed to cool naturally in a nitrogen atmosphere until room temperature.

The oven temperature was selected based on the melt profiles of the materials and to align with the usual practice of setting a powder pre-heat temperature below the melt range but above the crystallization temperature of the material.[9]

Characterization of molecular weight, melting and crystallization behavior, and rheological properties was conducted on each of the two materials at each duration of thermal aging (including a zero-aged control sample).

Molecular weight and structure

Molecular weight (MW) and structure were determined using the OMNISEC multi-detector size exclusion chromatography (SEC) system, including refractive index (RI) and UV-Vis PDA detectors, right angle or low angle light scattering (RALS/LALS), and the online differential viscometer detectors. The system was set up as follows: organic columns, mobile phase HFIP and 0.2 M potassium trifluoroacetate (KTFA), flow rate 0.7 mL/min, autosampler, column oven, and detector oven temperature, respectively, 20 °C, 40 °C, and 40 °C. System control, data acquisition, data analysis, and data reporting were performed using OMNISEC™ V11+ software.

SEC is a liquid chromatography method that separates macromolecules according to their size (hydrodynamic volume). The use of a multi-detector SEC system allows macromolecules to be characterized in terms of their absolute molecular weight and molecular weight distribution while providing additional information about molecular size and molecular structure. The RI and UV-Vis detectors are concentration detectors and provide a concentration profile of the sample eluted at a certain range of retention volume (RV). In this study, the RI detector was used and combined with RALS/LALS and a viscometer to fully characterize the samples.

A Mark-Houwink plot was produced in order to identify any structural differences between the different powders and ages. This is a double logarithmic plot of intrinsic viscosity (IV) against molecular weight; the IV indicates the density of a macromolecule in solution and will tend to increase linearly with increasing molecular weight if no change in structure is present. The M-H plot slope therefore relates to the macromolecule structure, while the intercept is indicative of the overall density.

Thermal properties

Differential scanning calorimetry (DSC) measurements were performed to analyze the melting and crystallization behavior of the different powders and printed samples. These values can be used to identify the relevant processing window for the high speed sintering, and other powdered-polymer AM processes. All tests were performed on a DSC 214 Polyma from Netzsch Analyzing & Testing (Selb, Germany), using Concavus pans, and a sample weight of 10 mg. Heating and cooling were performed at a rate of 10 °C/min in a nitrogen atmosphere. Two heating cycles were run for each sample in order to identify any inherent material changes following heating and crystallization.

Rheology

Oscillatory testing was used to study changes in viscoelastic behavior resulting from aging of the different powders and the observed increase in molecular weight. A Kinexus Ultra + rotational rheometer from Netzsch Analyzing & Testing (Selb, Germany) was used for this work. Disposable parallel plates with a 25 mm diameter (PP25) and a gap of 500 μm were employed. A shear strain of 1%, which was within the linear viscoelastic region, was used for all measurements. Frequency sweeps were performed at 200 °C over a range of 10^{-1}

to 10^2 Hz with the aim to study relaxation dynamics of the polymer melts. Temperature sweeps were also performed in order to study the cooling and crystallization behavior. Measurements were made between 200 °C and 30 °C at a frequency of 1 Hz and a cooling rate of 2 °C/min.

Sample production

Tensile test specimens were produced from each material at each level of aging, nominally providing six different 'grades' of material to test. Specimens were produced in an ambient air atmosphere using a voxeljet VX200 high-speed sintering system. The high speed sintering process works through a combination of infrared energy and an ink containing an infrared absorber, in this case carbon black. The ink is printed via an inkjet printhead onto the required cross-sections of the polymer powder; the difference in absorption between the printed and non-printed areas allows selective melting of the underlying material, creating the required part layer. The process continues by depositing and selectively printing consecutive layers of the part, with the unprinted material acting to support the parts throughout the build.

Five tensile test specimens were produced in a single layer of the build area. Build parameters were selected as shown in Table 1.

Each build was allowed to cool within the HSS machine for 1 h before being removed and allowed to cool to room temperature. Parts were removed and post-processed using glass beads in a Guyson Euroblast bead blaster in order to remove any loose powder.

Tensile testing

Tensile testing was carried out using a Tinius Olsen H5KS system with a laser extensometer. Testing was carried out in accordance with ASTM D638 at an extension rate of 5 mm/min.

Results

Molecular weight and structure

The RI and RALS chromatograms for the virgin and aged PA650 and PA615 powders are shown in Figure 1 in overlay plots of duplicate injections. For both polymers, the chromatograms shift toward lower RV when the sample is aged, indicating an increase in size. Generally, the LS detector responds to the sample molecular weight in addition to sample concentration, and hence here, at similar sample concentrations (similar intensities of RI chromatograms), the

Table 1. Build parameters used to produce HSS parts.

| Parameter	Description	Setting
Part bed temperature	Temperature at which the part bed is maintained throughout the build.	160 °C
Layer thickness	Thickness of each powder layer deposited by the recoating carriage.	0.1 mm
Recoat speed	Travel speed of the recoating carriage during powder deposition. Also the lamp's speed during preheating of the deposited powder.	70 mm/s
Preheat lamp power	Percentage of maximum power (1 kW) supplied to the lamp to preheat recently deposited powder.	50%
Ink density	Quantity of ink deposited on the regions to be sintered. (Number of droplets that combine to form each dot printed onto the part bed).	3 dots per drop (DPD)
Lamp speed	Travel speed of the lamp during sintering.	60 mm/s
Lamp power	Percentage of maximum power (1 kW) supplied to the lamp to sinter printed regions.	100%
Blank layers	Number of layers deposited prior to sintering, enabling the part bed temperature to stabilize before sintering.	100 layers
Finish Layers	Number of blank powder layers deposited on top of completed build.	10 layers
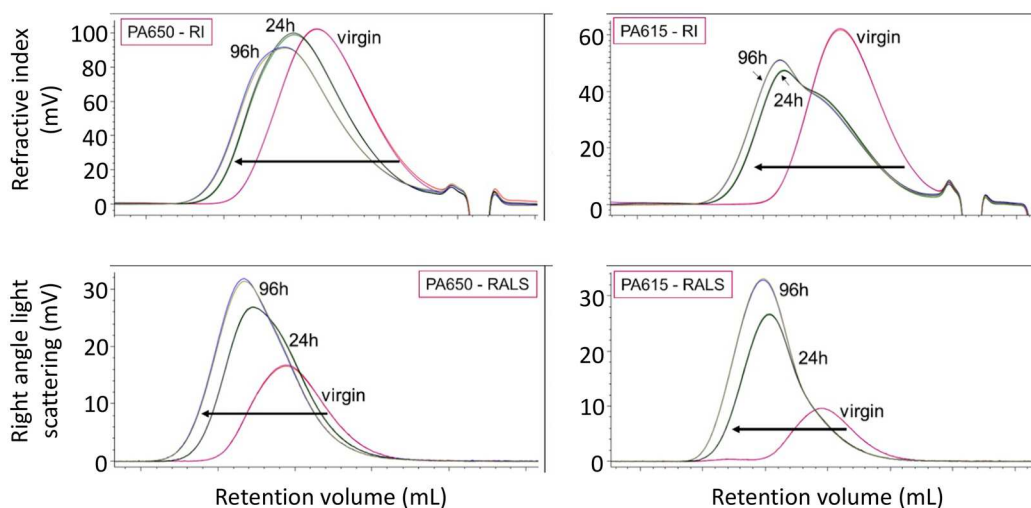
Figure 1. Overlaid RI (top) and RALS (bottom) chromatograms for duplicate injections of PA650 (left) and PA615 (right) powder samples at the different aging stages. Quantitative results can be found in Appendix 1 in the supplementary information.
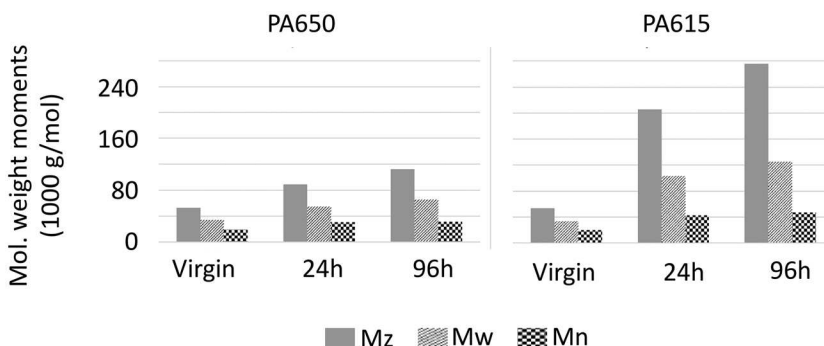

Figure 2. Comparison of molecular weight moments (Z-average, weight-average, and number-average molecular weight: Mz, Mw, and Mn) of PA650 (left) and PA615 (right) powders.

increase in LS intensity observed for all the aged samples indicates an increase in molecular weight. The RI chromatograms for aged PA615 show a shoulder at a lower retention volume that is not seen in the aged PA650 samples. This shoulder indicates the presence of at least two different populations with different sizes within the PA615 sample, suggesting an uneven aging process of the polymer chains within this sample.

Figure 2 presents the molecular weight moments for each powder at each level of aging. The virgin samples of PA650 and PA615 have very similar molecular weight distributions, suggesting that the nylon-12 used in the samples is, if not the same, very similar, and for both materials there is a clear increase in molecular weight with aging, especially in the Z-average molecular weight (Mz), which is biased toward larger molecular weight species and indicates a significant increase in the number of larger molecules with aging.

While both materials display similar trends, the observed increase in molecular weight is significantly greater in the case of the glass-filled nylon-12 (PA615), as can be seen graphically in Figure 2. An increase in dispersity (Đ) with aging, indicating a broader distribution of molecular weights, was also observed. This increase was more pronounced for the PA615 material; this, combined with the non-monotonic RI peak, supports the observation that the two materials age differently.

The Mark-Houwink plots (M-H) of the six samples (Figure 3) overlap perfectly and appear linear with no change of slope, indicating that no structural changes are occurring during aging.
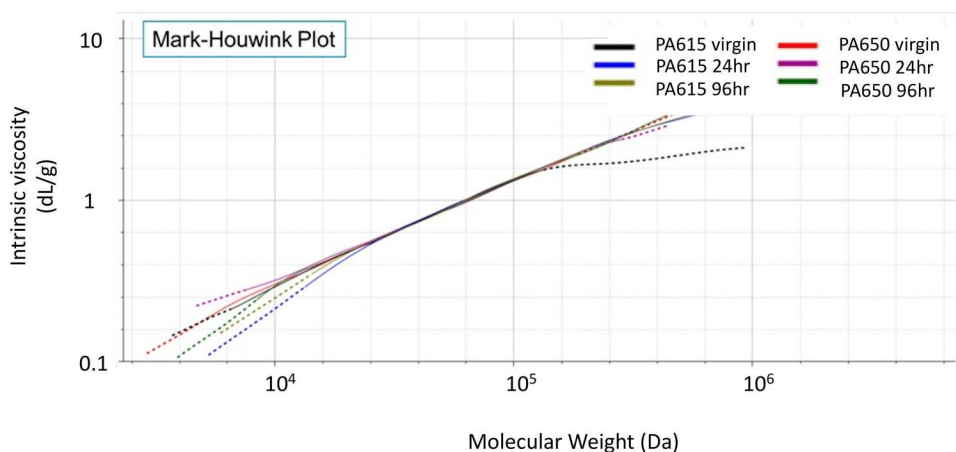
Figure 3. Mark-Houwink plot overlay of PA650 and P615 powder, virgin, and aged samples.

The mechanism of aging can therefore be hypothesized to be one of linear chain growth rather than branching, as observed by Wudy and Drummer[4] who attributed the aging mechanism, i.e., the increase in MW of the polymer chains, to solid-state polycondensation reactions.

Thermal properties

For both powders, the peak melt temperature, melt enthalpy, and crystallization temperature decreased with increasing aging time for the glass-filled powder (Figure 4), with a less significant temperature effect in the non-filled version. This is believed to be as a result of the increase in molecular weight observed with aging, leading to less densely packed spherulites and a subsequent decrease in crystallinity. This can be seen in the significant correlations between Mw and DSC data shown in Figure 5. The differences observed between the filled and unfilled powders may be attributed to local variation in glass content due to dry mixing and/or compositional differences in the specific PA12 used for each powder.

Rheology

Frequency sweeps show an increase in complex shear modulus (G*) with aging time (Figure 6), which is further confirmation that the molecular weight is increasing. The change is bigger from virgin to 24 h aged material than from 24 to 96 h of aging, indicating that the virgin material is most sensitive to aging. The same trend is observable with and without fillers; however, it is more pronounced with fillers. When plotted as G' and G" (Figure 7), the storage modulus and loss modulus, respectively, we also see a decrease in the crossover frequency. This represents an increase in relaxation time, meaning the polymers are more elastic due to their larger molecular weight and take longer to disentangle and relax.

The temperature sweeps (Figures 8 and 9) offer further insight into the cooling and crystallization behavior of the various samples. For virgin PA615 (glass-filled), the viscous modulus G" dominates before and during crystallization, whereas for the aged version of the same material, the elastic modulus G' dominates both before and during crystallization. This was also observable for the unfilled material, but to a smaller extent (see additional data in Appendix 3 of the supplementary information). This shows that the elastic behavior is more pronounced after aging, even at melt temperatures, indicating that the coalescence of powder particles will be reduced with increased aging time. On a molecular level, this may also indicate a higher degree of entanglement, which may hinder crystallization dynamics and potentially crystallite structure.
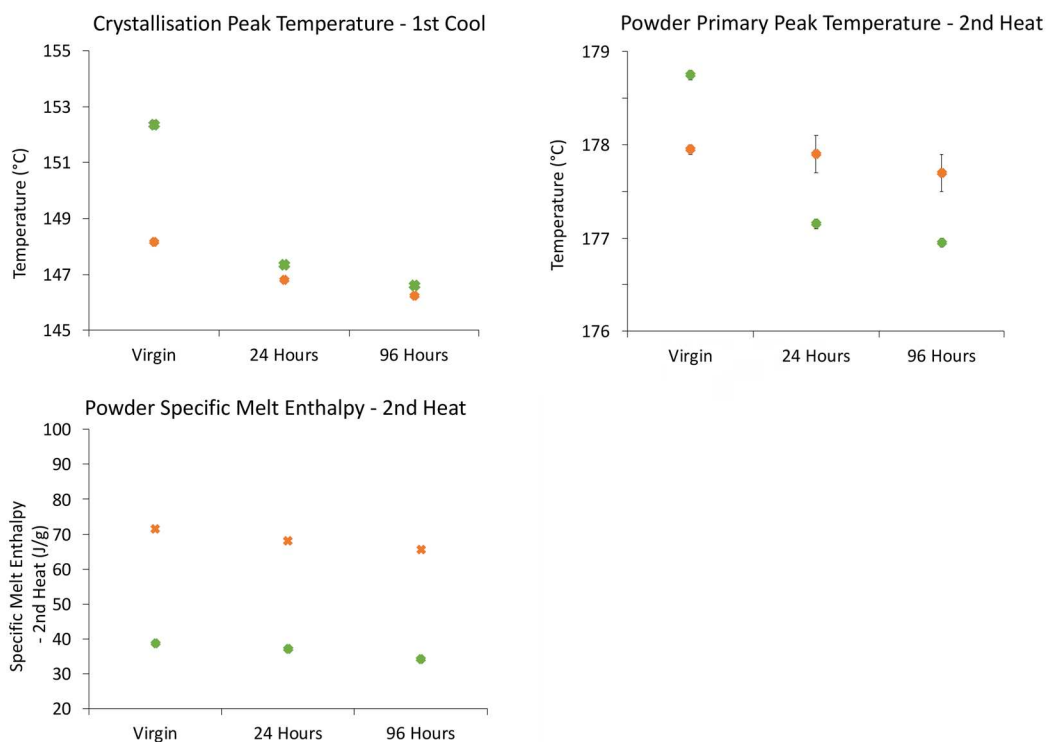
Figure 4. Analysis of the peak temperature of cooling and peak melt temperature and melt enthalpy[1] for the second heating cycle for all powders (**red** PA650, **green** PA615-GS) (additional data can be found in Appendix 2 in the Supplementary data).
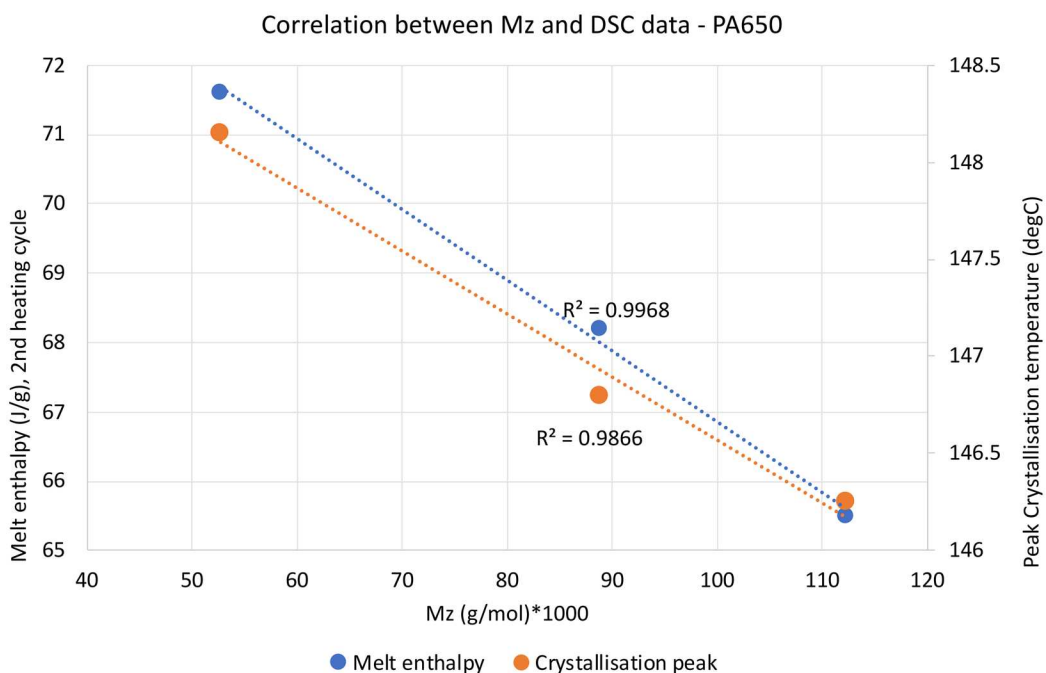

Figure 5. Correlation between Mz molecular weight data and thermal characteristics (melt enthalpy and peak crystallization temperature), showing a significant linear relationship between the relevant data-sets.
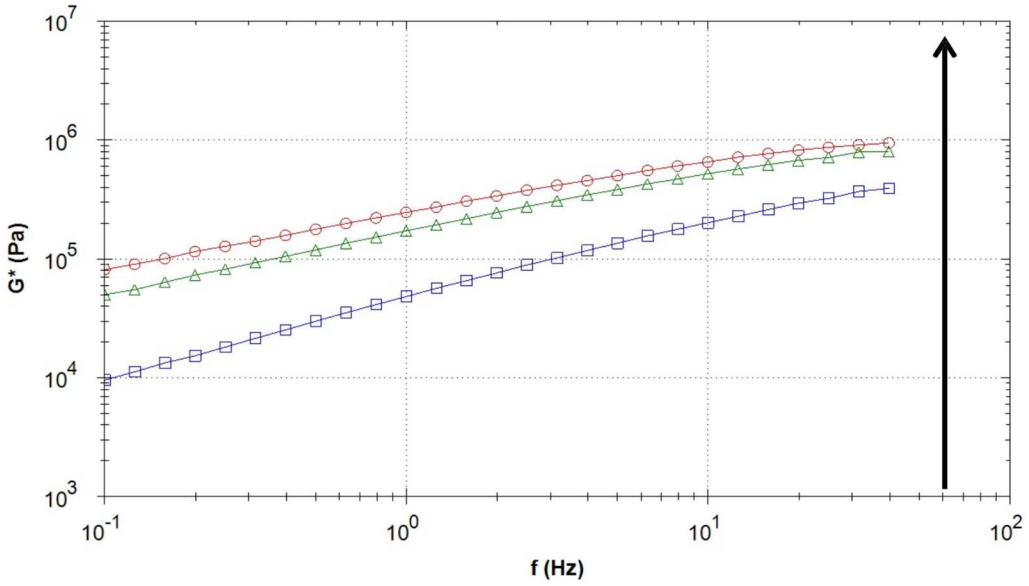
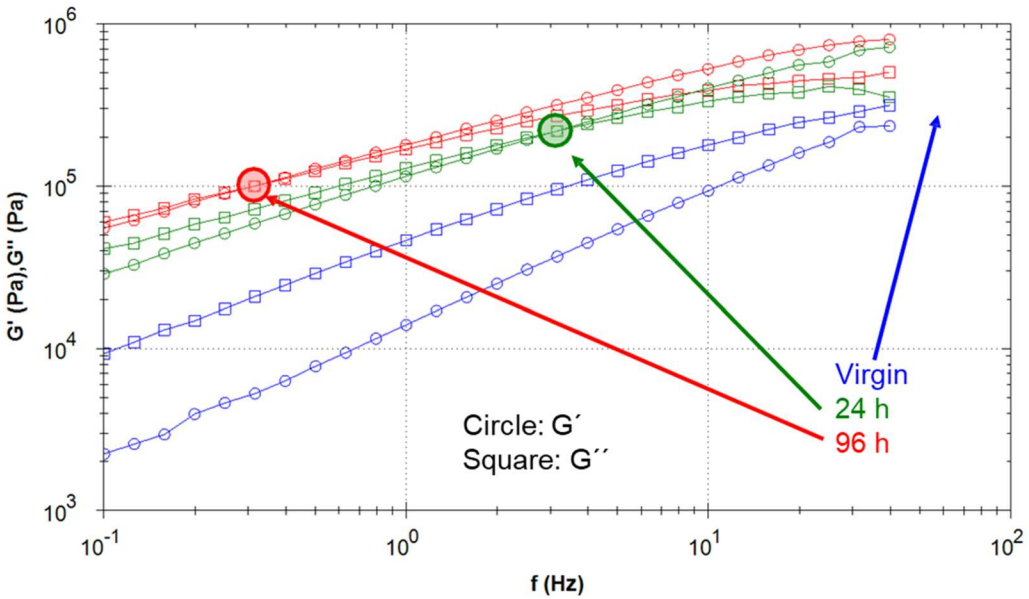**Figure 6.** Effect of aging time on complex shear modulus (G*) for PA615 (glass filled) powder samples.

Figure 7. Effect of aging time on storage modulus and loss modulus (G′ and G″) for PA615 (glass filled) powder samples.

Tensile testing

Tensile results for each material can be found in Figure 10. Note that, due to an unexpected machine failure, data is not available for 96-h aged PA615-GS; we recognize that this limits the conclusions that can be drawn regarding the effect of aging beyond 24 h on mechanical properties.

It can be seen that there is a decrease in ultimate tensile strength and Young's modulus with increasing age for each powder, likely caused by reduced bonding due to higher elasticity of the aged powders discussed earlier. Elongation at break increased with powder age, as would be expected based on previous literature. Full tabulated data can be found in Appendix 4.
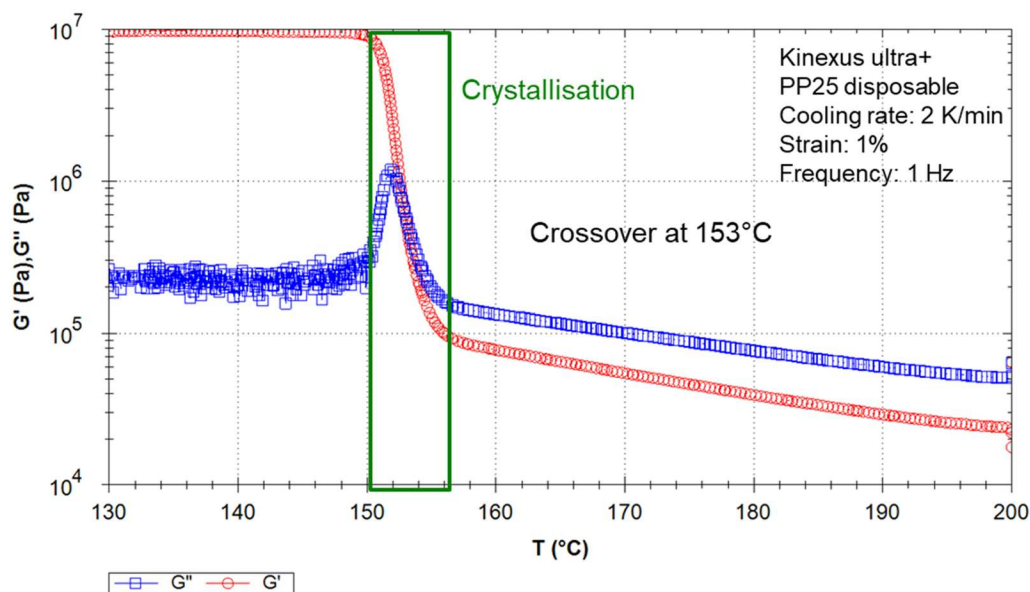
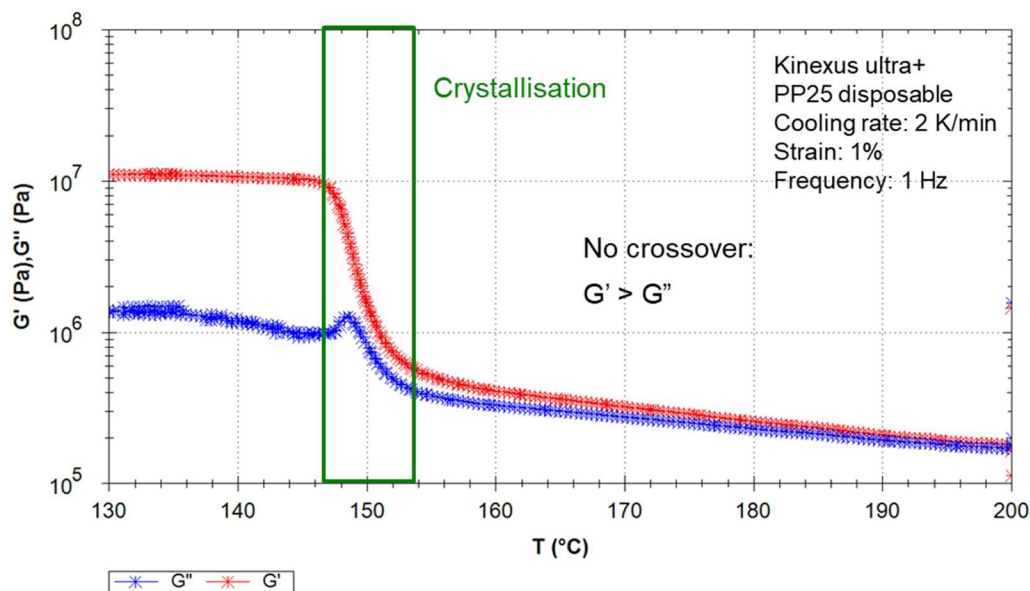**Figure 8.** Temperature sweep for virgin PA615 (glass-filled) material.

Figure 9. Temperature sweep for aged PA615 (glass-filled) material (96h).

Discussion

Effects of glass filler

The results presented here have demonstrated that the presence of glass filler does not significantly alter the aging trends observed. The SEC results demonstrate that both powders undergo an increase in molecular weight with aging, with an increase in the quantity of larger molecules, and no structural differences in either powder. This is as expected based on the literature discussed previously and the fact that the glass filler can be expected to be unchanged at the temperatures encountered during the heating process. However, these changes, along with the
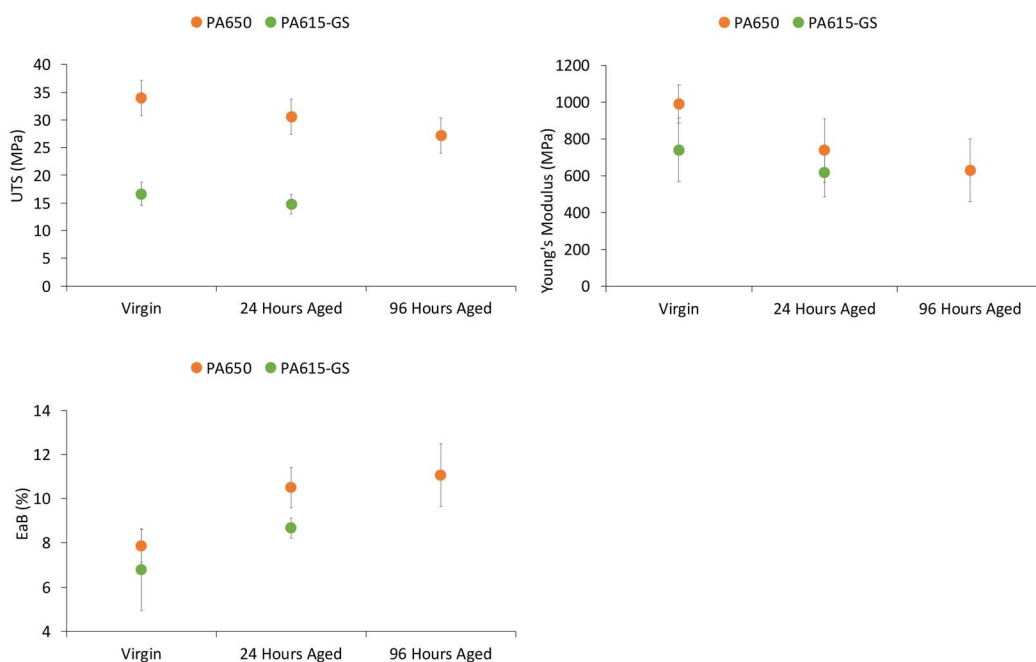
Figure 10. Effect of powder aging on tensile properties (PA650 and PA615-GS).

additional effects identified through DSC and rheometry, were seen to be much more pronounced in the glass-filled powder. These results suggest that either the glass filler leads to changes in the PA12 powder or that the base PA12 powder itself is different between the two batches.

In order to investigate this, a further study was performed on the two materials. The known difference between the two samples is the presence of the glass beads in PA615. PA615 contains *ca.* 50% of glass beads, as observed as well from the recoveries obtained by SEC (see Table in Appendix 1). Hence it was hypothesized that these glass beads could be the potential reason for the different aging process between the two samples. Note that the specific formulations of these materials were unspecified, but the sample composition is key to understanding the different behavior. However, in an attempt to investigate the hypothesis of the glass beads impacting the aging process, a second sample of PA615 was removed of the glass beads. A statically charged plastic 'card' was used to separate out the polymer particles from the virgin PA615 sample; these polymer samples were attracted to the charged card and collected, leaving the glass bead unaffected in the Petri dish.

Microscopy images (Figure 11) confirmed that the separation process had been mostly effective, with a small number of glass beads remaining in the samples but at insignificant proportions when compared with the unseparated PA615 GS.

The PA615 without glass beads, along with a second sample of PA650 and of PA615 "not-purified" as references, was aged in the same manner for 24 h, and all samples were analyzed by SEC. During sample preparation, a white deposit could be observed in both PA615 sample solutions (with and without the removal of the glass beads). This deposit was assumed to be the remaining glass beads.

Figure 12 demonstrates the MW moments obtained for these new samples. The same trends observed previously were also observed here, with the PA650 still showing a smaller increase in MW after aging compared to the non-purified PA615 sample. More interestingly, it can be seen that the results of the purified and non-purified PA615 samples showed very similar increases in molecular weight, indicating that the removal of the glass beads did not bring any substantial change. For the quantitative results, please see Appendix 1 in the supplementary information.

PA650   PA615-GS   PA615-GS with
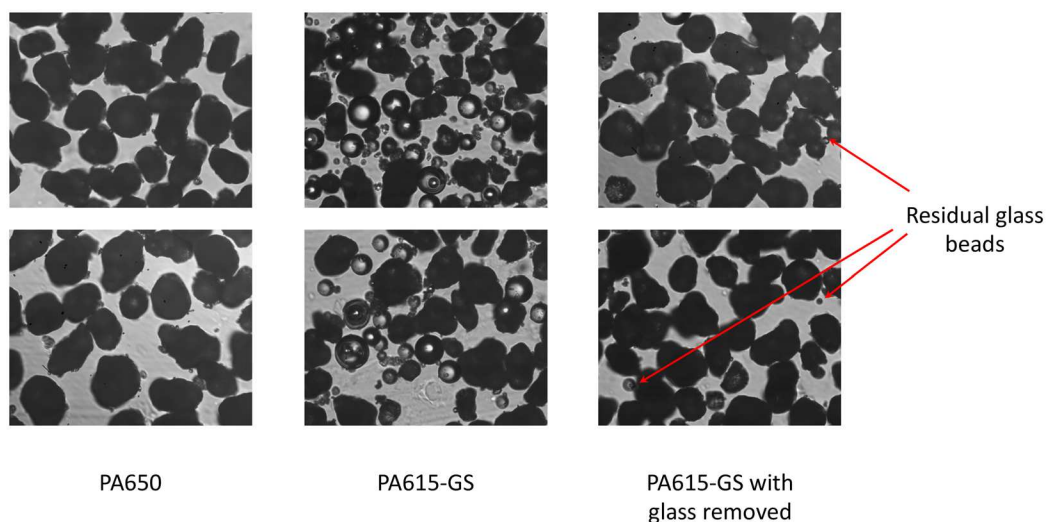   glass removed

Figure 11. Microscopy images of PA650, as-received PA615-GS and PA615-GS following removal of glass beads, demonstrating that minimal glass remains in the powder following the separation process.
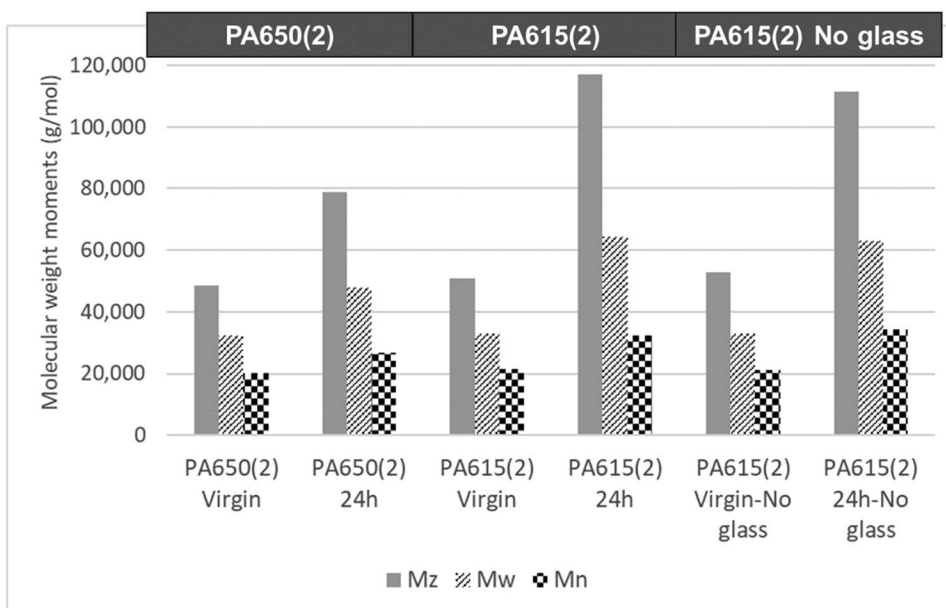

Figure 12. Comparison of molecular weight moments (Z-average, weight-average, and number-average molecular weight: Mz, Mw, and Mn) of the second (2) set of samples: PA650 and PA615 with and without glass beads.

This provides strong evidence that the changes in aging behavior observed between the two original materials are a result of differences in the base PA12 powder rather than the inclusion of the glass filler itself. Following this stage of the work, the manufacturer of the two materials confirmed that they do, in fact, contain different versions of PA12. Although the specific details of each material are to remain confidential, this provides further evidence of our hypothesis.

Practical implications of powder aging

The scientific findings presented in section "Results" can be related to specific processing effects in powdered-polymer additive manufacturing. The increase in molecular weight characteristics

observed with age can be related both to powder processibility, and recyclability; an increase in Molecular Weight is indicative of an increase in melt viscosity. This increase in melt viscosity can require modifications to processing parameters (e.g., slower sintering) in order to achieve consistent part quality and can require higher refresh ratios (proportion of virgin to reused material). Beyond a certain level, powder becomes practically unusable in these processes, leading to poor sintering and poor surface finish in addition to changes observed in mechanical properties. The more rapid increase in molecular weight for the PA615 powder suggests that this powder is likely to reach the end of its useful life significantly earlier than the PA650, with associated negative impacts in terms of cost and sustainability. The differences between the behavior of the two powders mean they are also likely to require different processing parameters at different ages in order to produce the required quality of parts.

The rheological tests conducted in section "Rheology" indicate that changes are induced in both materials once they have been held at elevated temperature, with subsequent changes less pronounced. This implies that, where repeatability of specific mechanical properties is required, virgin or "slightly used" powder should be prioritized over more highly used material.

The relatively large decrease in crystallization temperature with aging for the PA615 powder, when compared with much smaller changes in melt temperature, may provide some benefit in terms of extending the viable processing window for this material, which in turn could provide some benefits in the ability to tailor part properties through altering processing parameters.

Conclusion

This research has demonstrated that the filled and unfilled powders age in similar ways, with the inclusion of the glass not affecting the observed trends.

SEC analysis showed that the process of powder aging leads to an increase in molecular weight for both nylon-12 samples, with particular impact on the Mz value. The results suggest the formation of polymer chains of very high molecular weight, without undergoing structural modifications, as seen in previous literature focused on pure nylon 12.

Rheology temperature sweeps show that aged samples are more elastic at the onset of crystallization, which will likely influence crystallization dynamics and crystallite architecture. It is possible that this enhanced elasticity affects crystallite architecture, leading to the subsequent effects observed during tensile testing.

Of specific interest is the identification of different aging mechanisms within the glass filled and non-filled nylon-12 samples; virgin samples have very similar molecular weights and molecular weight distributions, whereas the aged samples show significant increases in the glass-filled, compared with the non-filled material. Frequency sweep measurements confirmed an increase in shear modulus and relaxation time for aged samples, also indicative of an increase in molecular weight.

Our results indicate that the glass filler itself is not the cause of this difference and that it is possible that the glass-filled material may contain a higher proportion of low molecular weight nylon-12, which may in turn affect the rate of polycondensation, although further work would be required in order to confirm this.

While the research presented here has focused on understanding powder aging, the principles and techniques used can be applied to powdered-polymer AM in a variety of other ways. These include testing of powders on delivery to establish any variations between batches of nominally identical material and testing the quality of powder from within the AM process(es) in order to maintain part quality while reducing waste.[]

Note

1. Normalized to account for the proportion of glass filler (50% weight percentage) in the PA615-GS material.

Disclosure statement

Funding

ORCID

Candice Majewski ⓘⅅ http://orcid.org/0000-0003-3324-3511

Data availability statement

Data is available upon request.

References

[1] Wohlers, T., I. Campbell, O. Diegel, J. Kowen, and N. Mostow. 2024. *Wohlers Report 2024: 3D Printing and Additive Manufacturing Global State of the Industry*. ASTM International, Washington, DC.

[2] Gornet, T. J., K. R. Davis, T. L. Starr, and K. M. Mulloy. 2002. "Characterization of selective laser sintering materials to determine process stability." In Solid freeform fabrication symposium proceedings, 2002, Austin, TX, pp. 546–53.

[3] Dotchev, K., and W. Yusoff. 2009. Recycling of polyamide 12 based powders in the laser sintering process. *Rapid Prototyp. J.* 15:192–203. doi:10.1108/13552540910960299

[4] Wudy, K., and D. Drummer. 2019. Ageing effects of polyamide 12 in selective laser sintering: molecular weight distribution and thermal properties. *Addit. Manuf.* 25:1–9. doi:10.1016/j.addma.2018.11.007

[5] Sanders, B., E. Cant, H. Amel, and M. Jenkins. 2022. The effect of physical aging and degradation on the Re-use of polyamide 12 in powder bed fusion. *Polymers.* 14:2682. doi:10.3390/polym14132682

[6] Pandelidi, C., R. Blakis, K. P. M. Lee, S. Bateman, M. Brandt, and M. Kajtaz. 2023. Thermal and oxidative aging effects of polyamide-11 powder used in multi-jet fusion. *Polymers.* 15:2395. doi:10.3390/polym15102395

[7] Stiller, T., M. Berer, A. D. Kashyap Katta, B. Haar, E. Truszkiewicz, W. Kraschitzer, H. Stepanvosky, G. Pinter, and J. M. Lackner. 2022. Powder ageing of polyamide 6 in laser sintering and its effects on powder and component characteristics. *Addit. Manuf.* 58:102987. doi:10.1016/j.addma.2022.102987

[8] Williams, R. J., L. Fox, and C. Majewski. 2021. The effect of powder age in high speed sintering of poly(pro-pylene). *Rapid Prototyp. J.* 27:707–719. doi:10.1108/RPJ-05-2020-0090

[9] Vasquez, M., B. Haworth, and N. Hopkinson. 2011. Optimum sintering region for laser sintered nylon-12. *Proc. Inst. Mech. Eng. Part B: J. Eng. Manuf.* 225(12):2240–2248.